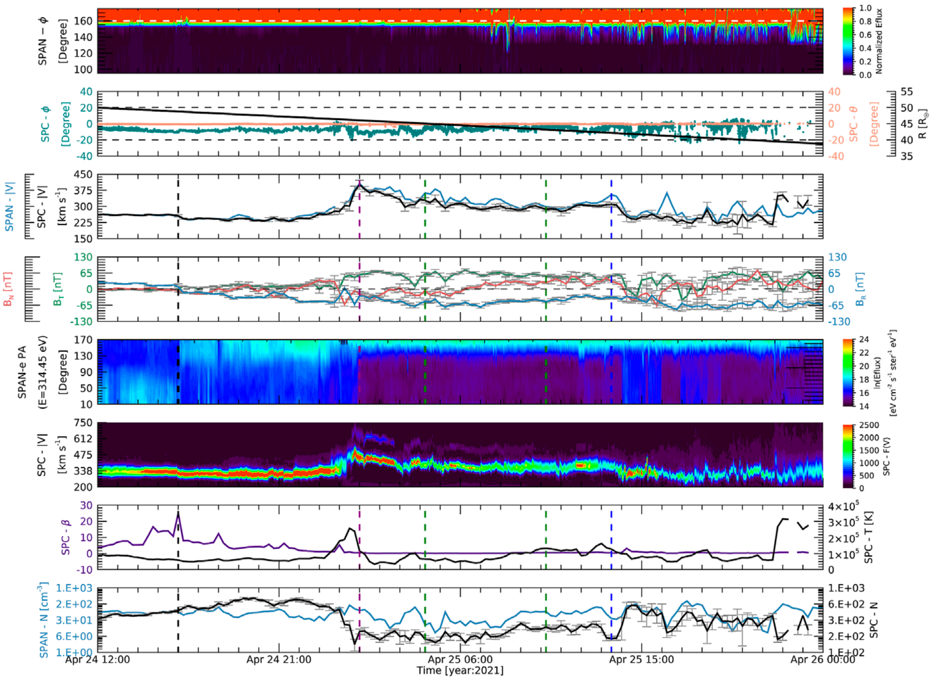


FIGURE 3
15-min resolution *in situ* data registered by PSP (SWEAP and FIELDS suites). From *top* to *bottom,* we show (first panel) the normalized energy flux distributions in function of SPAN-$\phi$-angle. During the event, most of the SPAN-distribution maxima were found when *SPAN*–$\phi > 160°$ (horizontal *white* dash line). In the second panel, we show the SPC-$\phi$ (in *teal*) and SPC-$\theta$ (in *peach*) flow angles. Due to cross-correlation between two plates of the Faraday's cup, we were not able to resolve SPC-$\theta$. Still, most of SPC-measurements were obtained with *SPC*–$\phi < |\pm 20°|$ (horizontal *black* dash lines). The PSP radial distance (R) to the Sun is overplot and shown in *black*. PSP was moving inbound when it registered the arrival of the prominence material at 46 $R_\odot$. In the third panel, we show both SPC-|*V*| (shown in *black*) and SPAN-|*V*| (in *gray*) proton speed and the magnitude of the magnetic field (|B| in *navy*). Next, we show the radial (R, in *blue*), tangential (T in *green*), and the normal (N in *red*) B components. In the fifth panel, the electron pitch angle (PA) for an energy of 314.45 eV with the color scale representing the logarithm of the energy flux vs. PA is shown. In the sixth panel, we show the SPC velocity distribution functions. Within 6 h after arrival, a second peak was clearly observed that remained constant for 12 h. Then, the SPC-$\beta$ parameter and proton temperature (SPC-T) are shown in the seventh panel, while in the last one, SPC-N and SPAN-N densities are shown. The structure is characterized by a sudden speed enhancement (reaching 400 km $s^{-1}$ and shown with a *purple* vertical line), followed by a constant speed region (300 km $s^{-1}$, *green* vertical lines) with no clear flux-rope configuration and ending with a structure at 310 km $s^{-1}$ (shown with a *blue* vertical line) but with no clear signatures of flux-rope configuration. The vertical *black* dash line shows the time where PSP crossed the heliospheric current sheet.

We also observed a clear and continuous $He^{2+}/H^{+} > 8\%$ ratio, that is, the presence of alpha-particles. The alpha-particle population is identified, in this case, from the clear secondary peak in the 1D reduced distribution functions (see *sixth* panel from Figure 3) from the SPC instrument (VDF, Case et al., 2020). The primary peak is, usually, associated with the core protons in the plasma, and it is well-measured throughout this period. The secondary peak is observed at roughly twice the kinetic-energy-per-charge of the proton core peak. This is often expressed in terms of the proton-equivalent speed, $V = \sqrt{Z/m}V_P$, where $Z$ and $m$ denote the charge number and mass number of the species. The second peak is most likely alpha-particles ($Z = 2$, m= 4) that are co-moving with protons, hence the apparent magnitude $V = \sqrt{2}V_P$.

Alternatively, a secondary peak might be associated with a proton beam component in the solar wind (Marsch et al., 1982; Alterman et al., 2018). In Figure 4, we present the 82-s time series of the alpha speed (*first* panel) and alpha ratio (*second*) estimated by SPAN's partial field of view. In the *third* panel, we show the alpha ratio computed with SPC. In the *fourth* panel, we present the magnetic field direction where $\phi_B$ is shown in *black* and $\theta_B$ in *blue*. In the *fifth* panel, we show $B_R/|B|$ (shown in *blue*) and SPC-$|V|$ for the VDF *first* ($V_1$) and *second* ($V_2$) peaks (in *black*) with the VDF maxima marked with *black* +. The VDF maxima were located computing the *first* and *second* derivatives of the VDF function.

In this case, we find the proton beam interpretation to be highly unlikely, as such secondary proton beams typically drift along the local magnetic field direction, relative to the core, with a drift speed that is at most on the order of the local Alfvén speed. Thus, the radial component of a proton distribution with a beam component would be expected to exhibit roughly Alfvénic or sub-Alfvénic drift speeds that modulate with the magnetic field angle. For the periods under consideration, the local Alfvén speed is roughly 100–200 km $s^{-1}$, which is comparable to the observed difference in the proton-equivalent speed and, coincidentally, to $\sqrt{2}V_P$. However, the apparent drift speed is not correlated with the magnetic field angle. We estimated a Pearson correlation coefficient of 0.46 between $V_2 - V_1$ and $B_R/|B|$, where $V_1$ and $V_2$ are the speeds of the *first* and *second* peaks on the VDF. We furthermore note that although the proton and alpha distributions are only partially measured by the SPAN instrument at this time, this experiment offers corroboration that the alpha component was significantly enhanced during this period (see *second* and *third* panels of Figure 4).